Homotopic Digital Rigid Motion: An Optimization Approach on Cellular Complexes

Nicolas Passat, Phuc Ngo, Yukiko Kenmochi

Homotopic Digital Rigid Motion: An Optimization Approach on Cellular Complexes*

Nicolas Passat[0000−0002−0320−4581]1, Phuc Ngo[0000−0002−7423−5932]2, and Yukiko Kenmochi[0000−0001−9648−326X]3

[1] Université de Reims Champagne Ardenne, CReSTIC EA 3804, 51097 Reims, France
[2] Université de Lorraine, LORIA, UMR 7503 Villers-lès-Nancy, France
[3] LIGM, Université Gustave Eiffel, CNRS, Marne-la-Vallée, France

Abstract. Topology preservation is a property of rigid motions in $\mathbb{R}^2$, but not in $\mathbb{Z}^2$. In this article, given a binary object $\mathsf{X} \subset \mathbb{Z}^2$ and a rational rigid motion $\mathcal{R}$, we propose a method for building a binary object $\mathsf{X}_{\mathcal{R}} \subset \mathbb{Z}^2$ resulting from the application of $\mathcal{R}$ on a binary object X. Our purpose is to preserve the homotopy-type between X and $\mathsf{X}_{\mathcal{R}}$. To this end, we formulate the construction of $\mathsf{X}_{\mathcal{R}}$ from X as an optimization problem in the space of cellular complexes with the notion of collapse on complexes. More precisely, we define a cellular space $\mathbb{H}$ by superimposition of two cubical spaces $\mathbb{F}$ and $\mathbb{G}$ corresponding to the canonical Cartesian grid of $\mathbb{Z}^2$ where X is defined, and the Cartesian grid induced by the rigid motion $\mathcal{R}$, respectively. The object $\mathsf{X}_{\mathcal{R}}$ is then computed by building a homotopic transformation within the space $\mathbb{H}$, starting from the cubical complex in $\mathbb{G}$ resulting from the rigid motion of X with respect to $\mathcal{R}$ and ending at a complex fitting $\mathsf{X}_{\mathcal{R}}$ in $\mathbb{F}$ that can be embedded back into $\mathbb{Z}^2$.

Keywords: rigid motions, Cartesian grid, homotopy-type, binary images, cubical complexes, cellular complexes.

1 Introduction

Rigid motions built by composition of rotations and translations are isometric transformations in the Euclidean spaces $\mathbb{R}^n$ ($n \geq 2$). In particular, they are bijective and they preserve geometric and topological properties between an object and its image. This is no longer the case when rigid motions are considered in the Cartesian grids $\mathbb{Z}^n$.

Translations [5, 19], rotations [1, 2, 6, 13, 27, 28, 31, 37] and more generally rigid motions [22–26, 29, 32] in the Cartesian grids have been studied with various purposes: describing the combinatorial structure of these transformations with respect to $\mathbb{R}^n$ vs. $\mathbb{Z}^n$ [5, 6, 19, 22, 30, 38], guaranteeing their bijectivity [1, 2, 13, 27, 31, 32, 37] or transitivity [28] in $\mathbb{Z}^n$, preserving geometrical properties [24, 25] and, less frequently, ensuring their topological invariance [23, 26] in $\mathbb{Z}^n$. These are non-trivial questions, and their difficulty increases with the dimension of the Cartesian grid [29]. Indeed, most of these works deal with $\mathbb{Z}^2$ [1, 2, 5, 6, 13, 19, 22, 23, 25–28, 32, 37]; fewer with $\mathbb{Z}^3$ [24, 31, 38].

* This work was supported by the French *Agence Nationale de la Recherche* (Grants ANR-15-CE23-0009 and ANR-18-CE23-0025).

In this article we investigate how it may be possible to preserve the topological properties of a digital object defined in the Cartesian grid when applying a rigid motion. In [26] a specific family of digital objects in $\mathbb{Z}^2$, called "regular", was proved to preserve their topology under any rigid motion. But all the digital objects in $\mathbb{Z}^2$ are not regular, and the required modifications for generating a regular object from a non-regular one induce asymmetric operations between the object and its background. In [23] the putative topology preservation between an object and its image in $\mathbb{Z}^2$ by a rigid motion was checked by searching a path in the combinatorial space of digital rigid motions [22] that corresponds to a point-by-point homotopic transformation between both. But this process allows to assess the topological invariance, not to ensure it.

We propose a new, alternative way of tackling the problem of digital rigid motion under the constraint of topological invariance. As in [23, 26], we consider the case of digital objects in $\mathbb{Z}^2$. Since a digital object X and its usual digital image by a rigid motion $\mathcal{R}$ are not guaranteed to present the same topology, our purpose is to compute a digital object $\mathsf{X}_\mathcal{R}$ that (1) has the same topology as X and (2) is "as similar as possible" to the usual digital image of X by $\mathcal{R}$. In other words, we accept to slightly relax some constraints on geometric similarity in order to ensure topological invariance. To reach that goal, we embed our digital objects in the Euclidean space and we process them in the (continuous but discrete) space of cellular complexes. This allows us to model / manipulate these objects in a way compliant with both their digital nature and their continuous interpretation (in particular from a topological point of view), but also to carry out basic transformations at a scale finer than that of $\mathbb{Z}^2$. The definition of $\mathsf{X}_\mathcal{R}$ from X and $\mathcal{R}$ is then formulated as an optimization problem, which presents similarities with the topology-preserving paradigms developed, for instance, in the framework of digital deformable models [10, 11, 36].

2 Problem Statement

Let $\mathsf{X} \subset \mathbb{Z}^2$ be a digital object. Let $X \subset \mathbb{R}^2$ be the continuous analogue of X, defined as $X = \mathsf{X} \oplus \square$ where $\oplus$ is the usual dilation operator [12] and $\square$ is the structuring element $[\frac{1}{2}, \frac{1}{2}]^2 \subset \mathbb{R}^2$. In other words, X is the union of the pixels (i.e. closed, unit squares) centered at the points of X. We note $\square : 2^{\mathbb{Z}^2} \to 2^{\mathbb{R}^2}$ the function that defines this continuous analogue, i.e. such that $\square(\mathsf{X}) = \mathsf{X} \oplus \square = X$.

Let $\mathcal{R} : \mathbb{R}^2 \to \mathbb{R}^2$ be a rigid motion, defined as the composition of a rotation and a translation. Usually, the image of the digital object $\mathsf{X} \subset \mathbb{Z}^2$ by the rigid motion $\mathcal{R}$, noted $\mathsf{X}_\mathcal{R}$ is a digital object of $\mathbb{Z}^2$ defined as $\mathsf{X}_\mathcal{R} = X_\mathcal{R} \cap \mathbb{Z}^2$, with $X_\mathcal{R} = \mathcal{R}(X) = \{\mathcal{R}(\mathbf{x}) \mid \mathbf{x} \in X\} \subset \mathbb{R}^2$. In other words, $\mathsf{X}_\mathcal{R}$ is defined as the Gauss digitization of the continuous object $X_\mathcal{R}$. We note $\boxdot : 2^{\mathbb{R}^2} \to 2^{\mathbb{Z}^2}$ the function that defines the Gauss digitization of a continuous object, i.e. such that $\boxdot(Y) = Y \cap \mathbb{Z}^2$. The usual overall process is exemplified in Fig. 1.

Our purpose is that $\mathsf{X}_\mathcal{R}$ be as similar as possible to X, up to the rigid motion $\mathcal{R}$. Reaching the best similarity can be formalized as solving the following optimization problem:

$$\mathsf{X}_\mathcal{R} = \arg_{\mathsf{Y} \subset \mathbb{Z}^2} \min \mathcal{D}_{\mathcal{R},\mathsf{X}}(\mathsf{Y}) \tag{1}$$

where $\mathcal{D}_{\mathcal{R},\mathsf{X}} : 2^{\mathbb{Z}^2} \to \mathbb{R}_+$ is an error measure (parameterized by $\mathcal{R}$ and X) that allows us to estimate the (dis)similarity between two digital objects. For instance, when considering

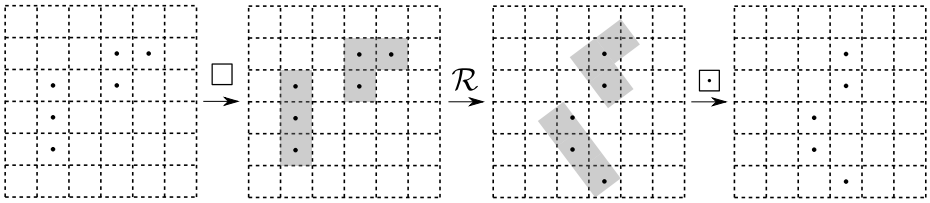

Fig. 1. Digitized rigid motion (here, by Gauss digitization). From left to right: $\mathsf{X} \subset \mathbb{Z}^2$, $X = \square(\mathsf{X}) \subset \mathbb{R}^2$, $\mathcal{R}(\square(\mathsf{X})) \subset \mathbb{R}^2$ and the result $\boxdot(\mathcal{R}(\square(\mathsf{X}))) = \mathsf{X}_\mathcal{R} \subset \mathbb{Z}^2$. (Dots: points of $\mathbb{Z}^2$; grey zones: parts of $\mathbb{R}^2$). This transformation does not preserve the topology between X and $\mathsf{X}_\mathcal{R}$.

the Gauss digitization we set $\mathcal{D}^{\boxdot}_{\mathcal{R},\mathsf{X}}(\mathsf{Y}) = |\, \boxdot\,(\mathcal{R}(\square(\mathsf{X}))) \setminus \mathsf{Y}\,| + |\,\mathsf{Y} \setminus \boxdot(\mathcal{R}(\square(\mathsf{X})))\,|$ and the unique solution $\mathsf{X}_\mathcal{R}$ is reached when $\mathcal{D}^{\boxdot}_{\mathcal{R},\mathsf{X}}(\mathsf{X}_\mathcal{R}) = 0$.

However, in this work, we also want to guarantee that $\mathsf{X}_\mathcal{R}$ has the same topology as X. In other words, we now want to solve the optimization problem (1) under an additional constraint that excludes the candidates $\mathsf{Y} \subset \mathbb{Z}^2$ that have a different topology from X. Still considering the Gauss digitization policy, a solution $\mathsf{X}_\mathcal{R}$ may then be reached for $\mathcal{D}^{\boxdot}_{\mathcal{R},\mathsf{X}}(\mathsf{X}_\mathcal{R}) > 0$, i.e. without fully satisfying the minimality requirements on the error measure. Our purpose is to solve this constrained optimization problem, i.e. to develop a method for computing the homotopic images of digital objects under rigid motions.

3 Hypotheses

Digital topology, adjacency – The digital objects of $\mathbb{Z}^2$ are considered in the usual framework of digital topology [35]. In this framework, an object X has to be considered with the 8- (resp. 4-) adjacency, whereas its background $\mathbb{Z}^2 \setminus \mathsf{X}$ is considered with the dual 4- (resp. 8-) adjacency, in order to avoid topological paradoxes related to the Jordan theorem [34]. Without loss of generality, we choose to consider $\mathsf{X} \subset \mathbb{Z}^2$ with the 8-adjacency (otherwise, it is sufficient to consider the complementary of X instead of X as the object).

Cellular / cubical complexes – In order to handle the digital-continuous analogy between the objects of $\mathbb{Z}^2$ and those of $\mathbb{R}^2$, we consider the (intermediate) framework of cellular complexes that was formalized in [15] in the case of cubical complexes induced by the Cartesian grid and proved compliant with both digital and continuous topologies [17, 20]. The cellular complexes can be generalized, without loss of generality to non-cubic partitions (see e.g. [7]), and in particular to partitions of $\mathbb{R}^2$ made of convex polygons.

Homotopy-type, simple points / cells – By "same topology", we mean that the objects we manipulate should have the same homotopy-type. This choice is relevant for two reasons. First, in dimension 2, the homotopy-type is equivalent to most of the other usual topological invariants. Second, there exist efficient topological tools that allow one to modify an object whereas preserving its homotopy-type. In particular, we will

rely on the notion of simple points / simple cells that are defined in the framework of digital topology and cubical complexes [9], and which can be extended without difficulty to any cellular complex thanks to the atomic notion of collapse [39].

Rational rigid motions – We define our rigid motions such that the translation and rotation parameters have rational values. In particular, the translation vectors will be defined on $\mathbb{Q}^2$ whereas the sine and cosine of the rotation angles will be defined from Pythagorean triples. This will allow us to handle a family of rigid motions sufficiently dense for actual applications [3], but with discrete parameters that will lead to exact calculus, thus avoiding any numerical approximation / error.

4 Rigid Motions

We first describe the transformations that we aim to study, namely the rigid motions composed of a rotation and a translation. In the sequel, a point of $\mathbb{R}^2$ will be noted in bold (e.g. $\mathbf{p}$) whereas its coordinates will be noted with subscripts x and y (e.g. $\mathbf{p} = (p_x, p_y)^t$). The transpose symbol will be omitted by abuse of notation (e.g. $\mathbf{p} = (p_x, p_y)$).

4.1 Basics on Rigid Motions

Let $\theta \in [0, 2\pi)$. Let $\mathbf{t} \in \mathbb{R}^2$. The rigid motion $\mathcal{R}_{(\theta,\mathbf{t})} : \mathbb{R}^2 \to \mathbb{R}^2$ is defined, for any $\mathbf{p} \in \mathbb{R}^2$ as:

$$\mathcal{R}_{(\theta,\mathbf{t})}(\mathbf{p}) = R(\theta) \cdot \mathbf{p} + \mathbf{t} \quad \text{where} \quad R(\theta) = \begin{bmatrix} \cos\theta & -\sin\theta \\ \sin\theta & \cos\theta \end{bmatrix} \tag{2}$$

is the rotation matrix of angle θ and $\mathbf{t}$ is the translation vector.

As stated in Sec. 3, we only consider rotation angles within the subset of $[0, 2\pi)$ that contains values built from Pythagorean triples [3], called rational rotations. More precisely, for any such θ, there exists a triple $(a, b, c) \in \mathbb{Z}^3$ such that $a^2 + b^2 = c^2$, that satisfies $\cos\theta = a/c$, $\sin\theta = b/c$ and $\tan\theta = b/a$. In other words, we have the guarantee that $\cos\theta$, $\sin\theta$ and $\tan\theta$ are rationals. In addition, we will also assume that $\mathbf{t} \in \mathbb{Q}^2$.

From now on, we will set $\alpha = \cos\theta = a/c$ and $\beta = \sin\theta = b/c \in [-1, 1] \cap \mathbb{Q}$ and the rotation matrix of Eq. (2) rewrites as:

$$R(\theta) = R(\alpha,\beta) = \begin{bmatrix} \alpha & -\beta \\ \beta & \alpha \end{bmatrix} = \frac{1}{c} \begin{bmatrix} a & -b \\ b & a \end{bmatrix} \tag{3}$$

The rigid motion $\mathcal{R}_{(\theta,\mathbf{t})}$ of Eq. (2), simply noted $\mathcal{R}$ from now on, can then be expressed from $(\alpha, \beta, t_x, t_y) \in \mathbb{Q}^4$, with $\alpha^2 + \beta^2 = 1$, and called rational rigid motions. In particular, for any $\mathbf{p} \in \mathbb{Q}^2$, we have:

$$\mathcal{R}(\mathbf{p}) = \begin{pmatrix} \alpha p_x - \beta p_y + t_x \\ \beta p_x + \alpha p_y + t_y \end{pmatrix} \in \mathbb{Q}^2 \tag{4}$$

4.2 Rigid Motion of a Digital Object

Let $\mathsf{X} \subset \mathbb{Z}^2$ be a digital object. Let $\mathcal{R} : \mathbb{Q}^2 \to \mathbb{Q}^2$ be a rational rigid motion such as defined by Eq. (4). Our purpose is to compute a digital object $\mathsf{X}_\mathcal{R} \subset \mathbb{Z}^2$ that corresponds to the image of X by $\mathcal{R}$, with regards to our two constraints, namely (1) the preservation of the homotopy-type between X and $\mathsf{X}_\mathcal{R}$, and (2) the optimality of $\mathsf{X}_\mathcal{R}$ with respect to the optimization problem (1).

In general, the object $\mathcal{R}(\mathsf{X}) = \{\mathcal{R}(\mathbf{x}) \mid \mathbf{x} \in \mathsf{X}\}$ does not fulfill the required properties. Indeed, by definition, we have $\mathcal{R}(\mathsf{X}) \subset \mathbb{Q}^2$, but in general we do not have $\mathcal{R}(\mathsf{X}) \subset \mathbb{Z}^2$. A usual solution consists of applying the rigid motion $\mathcal{R}$ on a continuous analogue of X. This continuous analogue is often chosen as $X = \square(\mathsf{X})$, i.e. by associating to each $\mathbf{x} \in \mathsf{X}$ the pixel centered on $\mathbf{x}$. We then obtain a continuous object $X \subset \mathbb{R}^2$, and we can relevantly build $X_\mathcal{R} = \mathcal{R}(X) = \{\mathcal{R}(\mathbf{x}) \mid \mathbf{x} \in X\}$. This object $X_\mathcal{R}$ has the same topology as X and thus as X [17, 20] but it is not defined in $\mathbb{Z}^2$. To define a digital object $\mathsf{X}_\mathcal{R}$ from $X_\mathcal{R}$, we generally rely on a digitization. But then, we can no longer guarantee that $\mathsf{X}_\mathcal{R}$ has the same topology as $X_\mathcal{R}$, X and X.

To tackle this issue, once $X_\mathcal{R} = \mathcal{R}(X) = \mathcal{R}(\square(\mathsf{X})) \subset \mathbb{R}^2$ has been built, we propose to transform it into another continuous object $Y \subset \mathbb{R}^2$, with three constraints: (1) the transformation between $X_\mathcal{R}$ and Y has to be homotopic; (2) Y may be the continuous analogue of a digital object of $\mathbb{Z}^2$, i.e. $Y = \square(\boxdot(Y))$; and (3) the digital object $\mathsf{Y} = \boxdot(Y) \subset \mathbb{Z}^2$ associated to Y may satisfy the optimality in Eq. (1) for the chosen measure $\mathcal{D}_{\mathcal{R},\mathsf{X}}$.

To reach that goal, we propose to work in the space of cellular complexes, that allows to model the continuous space $\mathbb{R}^2$ in a discrete way, but also to carry out homotopic transformations.

5 Cellular Complexes

We first recall definitions and notations on cellular complexes (Secs. 5.1, 5.2). There exist many ways for formalizing these notions. Without loss of generality, we choose those that allow us to describe our targeted cellular spaces (Secs. 5.3, 5.4).

5.1 Basics on Cellular Complexes

Let $P \subset \mathbb{R}^2$ be a closed, convex polygon. Let $\mathring{P}$ be the interior of P and $\partial P = P \setminus \mathring{P}$ the boundary of P. We note $\mathcal{P}(P) = \{\mathring{P}\}$. Let $E \subset \partial P$ be a maximal, closed line segment of ∂P. Let $\mathring{E}$ be the interior (i.e. the open line segment) of E, and $\partial E = E \setminus \mathring{E}$ be the boundary of E. The open line segment $\mathring{E}$ is called an edge of P. We note $\mathcal{E}(P)$ the set of all the edges of P. Let $\mathbf{v} \in \partial E$ be a point of ∂E; the singleton set $V = \{\mathbf{v}\}$ is called a vertex of P. We note $\mathcal{V}(P)$ the set of all the vertices of P. The set $\mathcal{F}(P) = \mathcal{P}(P) \cup \mathcal{E}(P) \cup \mathcal{V}(P)$ is a partition of P.

Let $\Omega \subset \mathbb{R}^2$ be a closed, convex polygon. Let $\mathcal{K}$ be a set of closed, convex polygons such that $\Omega = \bigcup \mathcal{K}$ and for any two distinct polygons $P_1, P_2 \in \mathcal{K}$, we have $\mathring{P}_1 \cap \mathring{P}_2 = \emptyset$. We set $\mathbb{K}(\Omega) = \bigcup_{P \in \mathcal{K}} \mathcal{F}(P)$. It is plain that $\mathbb{K}(\Omega)$ is a partition of Ω. We call $\mathbb{K}(\Omega)$, or simply $\mathbb{K}$, a cellular space (associated to Ω).

Each element $\mathfrak{f}_2$ (resp. $\mathfrak{f}_1$, resp. $\mathfrak{f}_0$) of $\mathbb{K}$ which is the interior (resp. an edge, resp. a vertex) of a polygon $P \in \mathcal{K}$ is called a 2-face (resp. 1-face, resp. 0-face). We set $\mathbb{K}_d$ ($0 \leq d \leq 2$, $d \in \mathbb{Z}$) the set of all the d-faces of $\mathbb{K}$. More generally, each element of $\mathbb{K}$ is called a face.

Let $\mathfrak{f} \in \mathbb{K}$ be a face. The cell $C(\mathfrak{f})$ induced by $\mathfrak{f}$ is the subset of faces of $\mathbb{K}$ such that $\bigcup C(\mathfrak{f})$ is the smallest closed set that includes $\mathfrak{f}$. If $\mathfrak{f}_0$ is a 0-face, then $C(\mathfrak{f}_0) = \{\mathfrak{f}_0\}$. If $\mathfrak{f}_1$ is a 1-face, then $C(\mathfrak{f}_1) = \{\mathfrak{f}_1, \mathfrak{f}_0^1, \mathfrak{f}_0^2\}$ with $\mathfrak{f}_0^1, \mathfrak{f}_0^2$ the two vertices bounding $\mathfrak{f}_1$, such that $\bigcup C(\mathfrak{f}_1)$ is a closed line segment. If $\mathfrak{f}_2$ is a 2-face, then $C(\mathfrak{f}_2) = \{\mathfrak{f}_2, \mathfrak{f}_1^1, \ldots, \mathfrak{f}_1^k, \mathfrak{f}_0^1, \ldots, \mathfrak{f}_0^k\}$ ($k \geq 3$) and $\bigcup C(\mathfrak{f}_2)$ is the closed polygon of interior $\mathfrak{f}_2$ with k edges $\mathfrak{f}_1^\star$ and k vertices $\mathfrak{f}_0^\star$. For any cell $C(\mathfrak{f})$, the face $\mathfrak{f}$ is called the principal face of $C(\mathfrak{f})$, and $C(\mathfrak{f})$ is also called the closure of $\mathfrak{f}$. The star $S(\mathfrak{f})$ of a face $\mathfrak{f}$ is the set of all the faces $\mathfrak{f}'$ such that $\mathfrak{f} \in C(\mathfrak{f}')$.

Remark A face $\mathfrak{f}$ and its induced cell $C(\mathfrak{f})$ are characterized by the list of the 0-faces in $C(\mathfrak{f})$. By abuse of notation, we will sometimes assimilate $\mathfrak{f}$ and $C(\mathfrak{f})$ to the sorted (e.g. clockwise) series of the k points $\mathbf{v}_i$ ($1 \leq i \leq k$) that correspond to these 0-faces $\{\mathbf{v}_i\}$.

A complex of $\mathbb{K}$ is a subset $K \subset \mathbb{K}$ defined as a union of cells of $\mathbb{K}$. The embedding of K into $\mathbb{R}^2$ is the set noted $\Pi_{\mathbb{R}^2}(K) \subset \mathbb{R}^2$ defined by $\Pi_{\mathbb{R}^2}(K) = \bigcup K$. Let $X \subset \mathbb{R}^2$. If there exists a complex $K \subset \mathbb{K}$ such that $X = \Pi_{\mathbb{R}^2}(K)$, then we say that K is the embedding of X into $\mathbb{K}$ and we note $K = \Pi_{\mathbb{K}}(X)$.

5.2 The Initial Cubical Space $\mathbb{F}$

The initial digital object X is defined in $\mathbb{Z}^2$, and so is the final digital object $\mathsf{X}_{\mathcal{R}}$ that we aim to build. Both have a continuous analogue in $\mathbb{R}^2$. The continuous analogue X of X is defined as $X = \square(\mathsf{X})$. The continuous analogue Y of $\mathsf{X}_{\mathcal{R}}$ is characterized by $Y = \square(\mathsf{X}_{\mathcal{R}})$ (see Sec. 4.2). In other words, both are defined as unions of unit, closed squares (i.e. pixels) centered on the points of X and $\mathsf{X}_{\mathcal{R}}$, respectively. In order to model / manipulate these two continuous objects X and Y of $\mathbb{R}^2$ as complexes, we build the cellular (actually, cubical) complex space $\mathbb{F}$ as follows.

Let $\Delta = \mathbb{Z} + \frac{1}{2} = \{k + \frac{1}{2} \mid k \in \mathbb{Z}\}$. Let $\delta \in \Delta$. We define the vertical line $V_\delta \subset \mathbb{R}^2$ and the horizon line $H_\delta \subset \mathbb{R}^2$ by the following equations, respectively:

$$(V_\delta) \quad x - \delta = 0 \tag{5}$$

$$(H_\delta) \quad y - \delta = 0 \tag{6}$$

We set $\mathscr{V}_\Delta = \{V_\delta \mid \delta \in \Delta\}$, $\mathscr{H}_\Delta = \{H_\delta \mid \delta \in \Delta\}$ and $\mathscr{G}_\Delta = \mathscr{V}_\Delta \cup \mathscr{H}_\Delta$. This set $\mathscr{G}_\Delta$ is the square grid that subdivides $\mathbb{R}^2$ into unit squares centered on the points of $\mathbb{Z}^2$. In other words, $\mathscr{G}_\Delta$ generates the Voronoi diagram of $\mathbb{Z}^2$ in $\mathbb{R}^2$.

The induced cellular complex space $\mathbb{F}(\mathbb{R}^2)$, simply noted $\mathbb{F}$, is then composed of:

- the set of 0-faces $\mathbb{F}_0 = \{\{\mathbf{d}\} \mid \mathbf{d} \in \Delta^2\}$;
- the set of 1-faces $\mathbb{F}_1 = \{]\mathbf{d}, \mathbf{d} + \mathbf{e}_x[\mid \mathbf{d} \in \Delta^2\} \cup \{]\mathbf{d}, \mathbf{d} + \mathbf{e}_y[\mid \mathbf{d} \in \Delta^2\}$; and
- the set of 2-faces $\mathbb{F}_2 = \{]\mathbf{d}, \mathbf{d} + \mathbf{e}_x[\times]\mathbf{d}, \mathbf{d} + \mathbf{e}_y[\mid \mathbf{d} \in \Delta^2\}$;

where $\mathbf{e}_x = (1, 0)$ and $\mathbf{e}_y = (0, 1)$. In particular, we have $\bigcup \mathbb{F}_0 = \mathscr{V}_\Delta \cap \mathscr{H}_\Delta$, $\bigcup \mathbb{F}_1 = \mathscr{G}_\Delta \setminus (\mathscr{V}_\Delta \cap \mathscr{H}_\Delta)$ and $\bigcup \mathbb{F}_2 = \mathbb{R}^2 \setminus \mathscr{G}_\Delta$.

For a digital object $\mathsf{X} \subset \mathbb{Z}^2$ and its continuous analogue $X = \square(\mathsf{X})$, we define the associated complex $F = \mathit{\Pi}_{\mathbb{F}}(X)$ as:

$$F = \bigcup_{\mathbf{x} \in \mathsf{X}} C(\blacksquare(\mathbf{x})) = \{\mathfrak{f} \in \mathbb{F} \mid \mathfrak{f} \subset X\} \tag{7}$$

where $\blacksquare : \mathbb{Z}^2 \to \mathbb{F}_2$ is the bijective function that maps each $\mathbf{p} \in \mathbb{Z}^2$ to the unit, open square (i.e. 2-face) $\blacksquare(\mathbf{p}) = \mathbf{p} \oplus]-\frac{1}{2}, \frac{1}{2}[^2$. We set $\mathbb{F}_d(F)$ $(0 \leq d \leq 2)$ the set of all the d-faces of F. In particular, we have:

$$X = \square(\mathsf{X}) = \bigcup \mathit{\Pi}_{\mathbb{F}}(X) = \mathit{\Pi}_{\mathbb{R}^2}(F) \tag{8}$$

$$\mathsf{X} = \boxdot(X) = \blacksquare^{-1}(\mathbb{F}_2(F)) \tag{9}$$

5.3 The Cubical Space $\mathbb{G}$ Induced by the Rigid Motion $\mathcal{R}$

The rigid motion $\mathcal{R}$ is applied on the continuous analogue $X \subset \mathbb{R}^2$ of X. The new continuous object $X_{\mathcal{R}} \subset \mathbb{R}^2$ is defined as $X_{\mathcal{R}} = \mathcal{R}(X) = \{\mathcal{R}(\mathbf{x}) \mid \mathbf{x} \in X\}$ (see Eq. (4)).

Similarly to X, that can be modeled by a complex F in the cubical space $\mathbb{F}$ defined in Sec. 5.2, the object $X_{\mathcal{R}}$ can also be modeled by a complex G in a cubical space $\mathbb{G}$. This second cubical space $\mathbb{G}$ is the image of $\mathbb{F}$ by the rigid motion $\mathcal{R}$. In particular, $\mathcal{R}$ trivially induces an isomorphism between these two cubical spaces.

More precisely, $\mathbb{G}$ derives from the square grid $\mathcal{R}(\mathscr{G}_\Delta)$ which subdivides $\mathbb{R}^2$ into unit squares centered on the points of $\mathcal{R}(\mathbb{Z}^2)$. We have $\mathcal{R}(\mathscr{G}_\Delta) = \mathcal{R}(\mathscr{V}_\Delta) \cup \mathcal{R}(\mathscr{H}_\Delta)$, with $\mathcal{R}(\mathscr{V}_\Delta) = \{\mathcal{R}(V_\delta) \mid \delta \in \Delta\}$ and $\mathcal{R}(\mathscr{H}_\Delta) = \{\mathcal{R}(H_\delta) \mid \delta \in \Delta\}$. For each $\delta \in \Delta$, the lines $\mathcal{R}(V_\delta)$ and $\mathcal{R}(H_\delta)$ are defined by the following equations, respectively:

$$(\mathcal{R}(V_\delta)) \qquad \alpha x + \beta y - \alpha t_x - \beta t_y - \delta = 0 \tag{10}$$

$$(\mathcal{R}(H_\delta)) \qquad -\beta x + \alpha y + \beta t_x - \alpha t_y - \delta = 0 \tag{11}$$

The induced cubical space $\mathbb{G}$ is then composed of the three sets of d-faces $\mathbb{G}_d = \mathcal{R}(\mathbb{F}_d) = \{\mathcal{R}(\mathfrak{f}) \mid \mathfrak{f} \in \mathbb{F}_d\}$ $(0 \leq d \leq 2)$.

The continuous object $X_{\mathcal{R}} \subset \mathbb{R}^2$ is then modeled by the complex $G = \mathit{\Pi}_{\mathbb{G}}(X_{\mathcal{R}}) \subset \mathbb{G}$:

$$G = \mathcal{R}(F) = \mathcal{R}(\mathit{\Pi}_{\mathbb{F}}(X)) = \{\mathcal{R}(\mathfrak{f}) \mid \mathfrak{f} \in \mathit{\Pi}_{\mathbb{F}}(X)\} \tag{12}$$

We set $\mathbb{G}_d(G)$ $(0 \leq d \leq 2)$ the set of all the d-faces of G.

5.4 The Cellular Space $\mathbb{H}$ Refining the Cubical Spaces $\mathbb{F}$ and $\mathbb{G}$

Although $X_{\mathcal{R}}$ presents good topological properties with respect to X, it cannot be directly used for building the final digital object $\mathsf{X}_{\mathcal{R}}$. Indeed, $X_{\mathcal{R}}$ is the continuous analogue of a digital object defined on $\mathcal{R}(\mathbb{Z}^2)$ but not $\mathbb{Z}^2$. In other words, the complex G that models $X_{\mathcal{R}}$ is defined on $\mathbb{G}$ and not on $\mathbb{F}$.

At this stage, our purpose is to build from the complex G in $\mathbb{G}$, a new cubical complex H in $\mathbb{F}$, that will be used to finally define the resulting digital object $\mathsf{X}_{\mathcal{R}}$. In order to guarantee the preservation of the homotopy-type between X and $\mathsf{X}_{\mathcal{R}}$, it is indeed necessary that G and H also have the same homotopy-type, i.e. we have to build H from G

via a homotopic transformation. This requires that these both complexes be defined in the same cellular space.

Then, we build a new cellular space $\mathbb{H}$ that refines both $\mathbb{F}$ and $\mathbb{G}$. This space $\mathbb{H}$ is not cubical; its 2-faces are convex polygons (with 3 to 8 edges). Practically, $\mathbb{H}$ is built from the subdivision of the Euclidean plane $\mathbb{R}^2$ by the union of the two square grids $\mathscr{G}_\Delta$ and $\mathcal{R}(\mathscr{G}_\Delta)$. In particular, for each 2-face $\mathfrak{h}_2$ of $\mathbb{H}$, there exists exactly one 2-face $\mathfrak{f}_2$ of $\mathbb{F}$ and one 2-face $\mathfrak{g}_2$ of $\mathbb{G}$ such that $\mathfrak{h}_2 = \mathfrak{f}_2 \cap \mathfrak{g}_2$. Based on this property, we define the two functions $\phi : \mathbb{H}_2 \to \mathbb{F}_2$ and $\gamma : \mathbb{H}_2 \to \mathbb{G}_2$, such that $\phi(\mathfrak{h}_2) = \mathfrak{f}_2$ and $\gamma(\mathfrak{h}_2) = \mathfrak{g}_2$. Reversely, we build the two functions $\Phi : \mathbb{F}_2 \to 2^{\mathbb{H}_2}$ and $\Gamma : \mathbb{G}_2 \to 2^{\mathbb{H}_2}$ such that for any $\mathfrak{f}_2 \in \mathbb{F}_2$ and $\mathfrak{g}_2 \in \mathbb{G}_2$, we have $\Phi(\mathfrak{f}_2) = \phi^{-1}(\{\mathfrak{f}_2\}) = \{\mathfrak{h}_2 \in \mathbb{H}_2 \mid \phi(\mathfrak{h}_2) = \mathfrak{f}_2\}$ and $\Gamma(\mathfrak{g}_2) = \gamma^{-1}(\{\mathfrak{g}_2\}) = \{\mathfrak{h}_2 \in \mathbb{H}_2 \mid \gamma(\mathfrak{h}_2) = \mathfrak{g}_2\}$.

The algorithmic process for building $\mathbb{H}$ from $\mathbb{F}$ and $\mathbb{G}$ is detailed in Appendix. This process can be carried out using only exact calculus since all the 0-faces of $\mathbb{H}$ have rational coordinates. Indeed, from Eqs. (5,6,10,11) the lines of $\mathscr{G}_\Delta$ and $\mathcal{R}(\mathscr{G}_\Delta)$ have rational-coefficient equations. In particular, for two (non-colinear) such lines L_i ($1 \leq i \leq 2$) of equations $a_i x + b_i y + c_i = 0$ ($a_i, b_i, c_i \in \mathbb{Q}$), the putative point of intersection $\mathbf{d}$ between both forming a 0-face $\{\mathbf{d}\}$ of $\mathbb{H}$ has the following coordinates:

$$d_x = \frac{b_1 c_2 - b_2 c_1}{a_1 b_2 - a_2 b_1} \in \mathbb{Q} \text{ and } d_y = \frac{a_1 c_2 - a_2 c_1}{a_2 b_1 - a_1 b_2} \in \mathbb{Q} \tag{13}$$

Based on the above functions, each complex F on $\mathbb{F}$ (resp. G of $\mathbb{G}$) can be embedded into $\mathbb{H}$ be defining a complex $\Pi_{\mathbb{H}}(F)$ (resp. $\Pi_{\mathbb{H}}(G)$) as $\Pi_{\mathbb{H}}(F) = \bigcup_{\mathfrak{f}_2 \in \mathbb{F}_2(F)} \bigcup_{\mathfrak{h}_2 \in \Phi(\mathfrak{f}_2)} C(\mathfrak{h}_2)$ (resp. $\Pi_{\mathbb{H}}(G) = \bigcup_{\mathfrak{g}_2 \in \mathbb{G}_2(G)} \bigcup_{\mathfrak{h}_2 \in \Gamma(\mathfrak{g}_2)} C(\mathfrak{h}_2)$), and we say that $\Pi_{\mathbb{H}}(F)$ (resp. $\Pi_{\mathbb{H}}(G)$) is the embedding of F (resp. G) in $\mathbb{H}$. For any complex H on $\mathbb{H}$, if there exists a complex F on $\mathbb{F}$ (resp. G on $\mathbb{G}$) such that $H = \Pi_{\mathbb{H}}(F)$ (resp. $H = \Pi_{\mathbb{H}}(G)$), then we write $F = \Pi_{\mathbb{F}}(H)$ (resp. $G = \Pi_{\mathbb{G}}(H)$) and we say that F (resp. G) is the embedding of H in $\mathbb{F}$ (resp. $\mathbb{G}$). In such case, we have in particular $\Pi_{\mathbb{F}}(H) = \bigcup_{\mathfrak{h}_2 \in \mathbb{H}_2(H)} C(\phi(\mathfrak{h}_2))$ (resp. $\Pi_{\mathbb{G}}(H) = \bigcup_{\mathfrak{h}_2 \in \mathbb{H}_2(H)} C(\gamma(\mathfrak{h}_2))$).

6 Optimization-Based Rigid Motion

We are now ready to describe the process that will allow us to define the digital object $\mathsf{X}_{\mathcal{R}}$. By contrast to the process depicted in Fig. 1, that does not handle topological constraints, the proposed approach, summarized in Fig. 2 aims to guarantee that X and $\mathsf{X}_{\mathcal{R}}$ will have the same topology.

The first four steps of this process (from X to H) and the last three ones (from $\widehat{H}$ to $\mathsf{X}_{\mathcal{R}}$) can be dealt with by considering Secs. 4 and 5 (keep in mind that all these steps are topology-preserving). The only part that remains to be described is the construction of the transformation $\mathfrak{H}$ from H to $\widehat{H}$. In particular, it is mandatory that:

- $\mathfrak{H}$ be a homotopic transformation (to preserve the topology between X and $\mathsf{X}_{\mathcal{R}}$);
- $\widehat{H}$ can be embedded into $\mathbb{F}$ (i.e. $\widehat{F} = \Pi_{\mathbb{F}}(\widehat{H})$ exists); and
- the digital analogue $\boxdot(\Pi_{\mathbb{R}^2}(\widehat{H})) \subset \mathbb{Z}^2$ of $\widehat{H}$ be a as close as possible to the exact solution of the optimization problem (1).

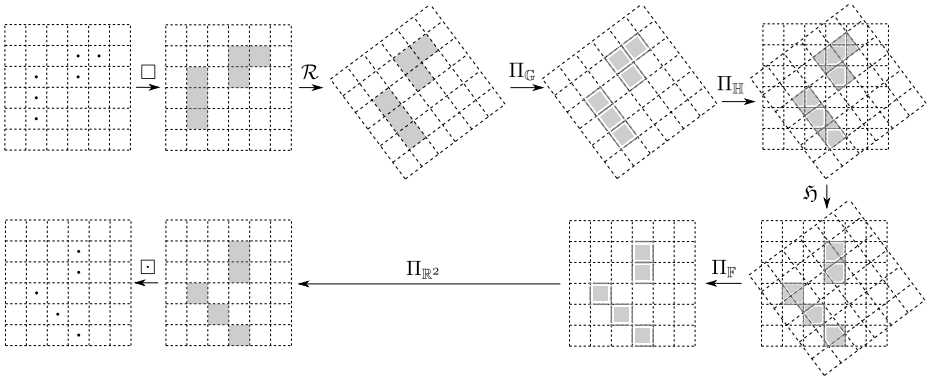

Fig. 2. Proposed framework for homotopy-type preserving rigid motion. Following the flowchart: $\mathsf{X} \subset \mathbb{Z}^2$, $\square(\mathsf{X}) = X \subset \mathbb{R}^2$, $\mathcal{R}(X) = X_{\mathcal{R}} \subset \mathbb{R}^2$, $\Pi_{\mathbb{G}}(X_{\mathcal{R}}) = G \subset \mathbb{G}$, $\Pi_{\mathbb{H}}(G) = H \subset \mathbb{H}$, $\mathfrak{H}(H) = \widehat{H} \subset \mathbb{H}$, $\Pi_{\mathbb{F}}(\widehat{H}) = \widehat{F} \subset \mathbb{F}$, $\Pi_{\mathbb{R}^2}(\widehat{F}) = Y \subset \mathbb{R}^2$ and $\boxdot(Y) = \mathsf{X}_{\mathcal{R}} \subset \mathbb{Z}^2$.

Algorithm 1: Definition of $\widehat{H}$ by construction of $\mathfrak{H}$.

Input: $H \subset \mathbb{H}$, $\mathcal{D}_{\mathcal{R},\mathsf{X}} : 2^{\mathbb{Z}^2} \to \mathbb{R}_+$
Output: $\widehat{H} \subset \mathbb{H}$

1 $\mathcal{D}_{cur} \leftarrow +\infty$
2 $\widehat{H} \leftarrow H$
3 **repeat**
4 $\quad \mathcal{D}_{ref} \leftarrow \mathcal{D}_{cur}$
5 $\quad$ **repeat**
6 $\quad\quad$ choose a face $\mathfrak{f} \in \mathbb{H}_2$ such that $C(\mathfrak{f})$ is simple for $\widehat{H}$
7 $\quad\quad$ **if** $\mathfrak{f} \in \widehat{H}$ **then** $\widehat{H} \to \widehat{H} \ominus C(\mathfrak{f})$ `//Remove the simple cell` $C(\mathfrak{f})$ `from` $\widehat{H}$
8 $\quad\quad$ **else** $\widehat{H} \to \widehat{H} \cup C(\mathfrak{f})$ `//Add the simple cell` $C(\mathfrak{f})$ `to` $\widehat{H}$
9 $\quad$ **until** $\Pi_{\mathbb{F}}(\widehat{H})$ exists
10 $\quad \mathcal{D}_{cur} \leftarrow \mathcal{D}_{\mathcal{R},\mathsf{X}}(\boxdot(\Pi_{\mathbb{R}^2}(\widehat{H})))$
11 **until** $\mathcal{D}_{cur} > \mathcal{D}_{ref}$

The construction of $\mathfrak{H}$ is formalized in Alg. 1. This algorithm is designed to iteratively modify H by "adding" or "removing" 2-cells until reaching the complex $\widehat{H}$ assumed to fulfill the required properties. Three points are important in this algorithm. First (Line 6), the choice of the 2-cells is constrained by their simplicity (Sec. 6.1). This guarantees that the transformation $\mathfrak{H}$, namely the whole sequence of these additions / removals is homotopic. Second (Line 9), it is mandatory that candidate complexes can be embedded in $\mathbb{F}$, and then in $\mathbb{Z}^2$. This is guaranteed by only checking the intermediate complexes that satisfy this property (which justifies the presence of a second loop into the first one). Third (Line 11), the process keeps searching candidate complexes while it is able to decrease the error measure. Alg. 1 is, of course, a very simplified framework that can be adapted / enriched according to the desired application.

6.1 Homotopic Transformations and Simple Cells in the Cellular Space

To guarantee that $\mathfrak{H}$ is a homotopic transformation, it is built as a sequence of additions / removals of simple cells. This notion of simple cell is directly derived from that considered in [9] which relies on the notion of collapse in complexes [39].

Let K be a complex defined in a cellular space $\mathbb{K}$ on $\mathbb{R}^2$. Let $\mathfrak{f}_2$ be a 2-face of K. Let $D_0(\mathfrak{f}_2)$ (resp. $D_1(\mathfrak{f}_2)$) be the subset of $C(\mathfrak{f}_2)$ composed by the 0- (resp. 1-) faces $\mathfrak{f}$ the star of which intersects K only within $C(\mathfrak{f}_2)$, i.e. $S(\mathfrak{f}) \cap K = S(\mathfrak{f}) \cap C(\mathfrak{f}_2)$. We say that $C(\mathfrak{f}_2)$ is a simple 2-cell (for K) if $|D_1(\mathfrak{f}_2)| = |D_0(\mathfrak{f}_2)| + 1$ (which is equivalent to say that the intersection of the border of $C(\mathfrak{f}_2)$ and K is connected and with a Euler characteristics of 1). In such case, the detachment (Line 7) of this 2-cell $C(\mathfrak{f}_2)$ from K, i.e. the operation that transforms K into $K \oslash C(\mathfrak{f}_2) = K \setminus (\{\mathfrak{f}_2\} \cup D_1(\mathfrak{f}_2) \cup D_0(\mathfrak{f}_2))$ corresponds to a collapse operation from K to $K \oslash C(\mathfrak{f}_2)$, and both complexes have the same homotopy-type. Reversely, if $\mathfrak{f}_2$ is a 2-face of $\mathbb{K} \setminus K$, and if $C(\mathfrak{f}_2)$ is a simple 2-cell for the complex $K \cup C(\mathfrak{f}_2)$, then the operation of attachment that transforms K into $K \cup C(\mathfrak{f}_2)$ corresponds to the inverse collapse operation from K into $K \cup C(\mathfrak{f}_2)$, and both complexes also have the same homotopy-type.

6.2 Solving the Optimization Problem: Discussion and Heuristics

Even if we consider a finite part of $\mathbb{Z}^2$ (which is the case in digital imaging), the induced finite space of the solutions of the optimization problem (1) is huge, and the topological constraints induced by the homotopy-type equivalence between X and $\mathsf{X}_{\mathcal{R}}$ are not sufficient to reduce this space to a tractable size allowing for an exhaustive investigation. Thus, we do not aim at solving exactly the optimization problem (1) (although we will sometimes succeed), but to find a solution reasonably close to the optimum. In particular, we only explore a part of the space of solutions. Our purpose is then to make this exploration as relevant as possible. We briefly discuss hereafter a non-exhaustive list of ideas that can be relevant to reach that goal.

Border processing – In general, the complex H cannot be directly embedded into $\mathbb{F}$. However, some parts of H already correspond to 2-cells of $\mathbb{F}$. In most cases, these parts that constitute the "internal" part of H will not be modified during the optimization process. More formally, this means that in most application cases, the addition / removal of simple 2-cells to / from H will occur for 2-faces $\mathfrak{f}_2$ such that $\Phi(\mathfrak{f}_2)$ intersects—but is not included in—H. In other words, it is generally sufficient to work on the "border" of H to build $\widehat{H}$ and thus $\widehat{F}$.

Measure separability and gradient climbing – Most error measures aim to emulate the behaviour of usual digitization policies. For instance the two ones considered in our experiments (Sec. 7) correspond to the Gaussian (Eq. (14)) and the majority vote (Eq. (15)) digitizations. From these very definitions, it is plain that it is possible to process the internal repeat loop (Lines 5–9) of Alg. 1 in order to deal with 2-cells of $\mathbb{F}$ (in particular the "border" ones) one after another, either by addition or removal of 2-cells of $\mathbb{H}$. In this context, it may be relevant to process them by giving the highest priority to the cells that induce the lowest increase of the metric error, following a (reverse)

gradient climbing paradigm.

Homotopic transformations in $\mathbb{F}$ – At the end of the first iteration of the external loop (Lines 3–11), a first complex $\widehat{H}$ has been built, and is such that $\widehat{F} = \Pi_{\mathbb{F}}(\widehat{H})$. Since the next occurrence of $\widehat{H}$ also has to satisfy this property, the next iterations of this loop can then work directly in $\mathbb{F}$ and no longer in $\mathbb{H}$.

Convergence issues – For most objects, the process converges in one iteration of the external loop. For the other objects, in particular those presenting complex details, several iterations may be required. However, for very complex objects, it may happen that the most internal loop may not end. This may be caused by the non-existence of a solution (under the topological constraints) in the context of a finite support image. This problem may be tackled by multigrid paradigm, for instance by considering $(\frac{1}{2}\mathbb{Z})^2$ instead of $\mathbb{Z}^2$ as output space.

7 Experiments

In this section, we illustrate the results that can be obtained with the proposed method.

We consider the two following error measures:

$$\mathcal{D}^{\boxdot}_{\mathcal{R},\mathsf{X}}(\mathsf{Y}) = |\, \boxdot\, (\mathcal{R}(\square(\mathsf{X}))) \setminus \mathsf{Y}\,| + |\, \mathsf{Y} \setminus \boxdot(\mathcal{R}(\square(\mathsf{X})))\,| \tag{14}$$

$$\mathcal{D}^{\square}_{\mathcal{R},\mathsf{X}}(\mathsf{Y}) = |\, \mathcal{R}(\square(\mathsf{X})) \setminus \square(\mathsf{Y})\,| + |\, \square(\mathsf{Y}) \setminus \mathcal{R}(\square(\mathsf{X}))\,| \tag{15}$$

where $|\cdot|$ is the cardinal for discrete sets (Eq. (14)), and the area for continuous objects (Eq. (15)). The first (resp. the second) corresponds to the Gauss (resp. majority vote) digitization. This will allow us to compare the results obtained by our method with these two usual digitization policies.

Results are illustrated in Fig. 3. They are proposed for small, yet complex objects. Indeed, we focus on objects that present details which are the most likely to be topologically altered by a rigid motion, namely small connected components and thin structures.

The first image (ellipse) is proposed to illustrate the fact that in the most simple cases (here an object without complex details and a globally smooth border), our method provides the same results as usual transformations-by-digitization approaches. Indeed, when such methods do not alter the topology, our method is assumed to have the same behaviour. It is also observed that the result using Eq. (15) has the smoother boundary than that using Eq. (14).

In the other three examples (head, circles and DGMM logo), the transformations-by-digitization (second and fourth columns) fail to preserve the topology, leading e.g. to breaking or merging connected components. By contrast, our method (third and fifth columns) succeed in preserving the topology, whereas leading to results with as few as possible differences with the transformations-by-digitization results.

8 Conclusion

The proposed approach of rigid motion for digital objects allows us to ensure topological invariance between the initial object and its image. This approach relies on an

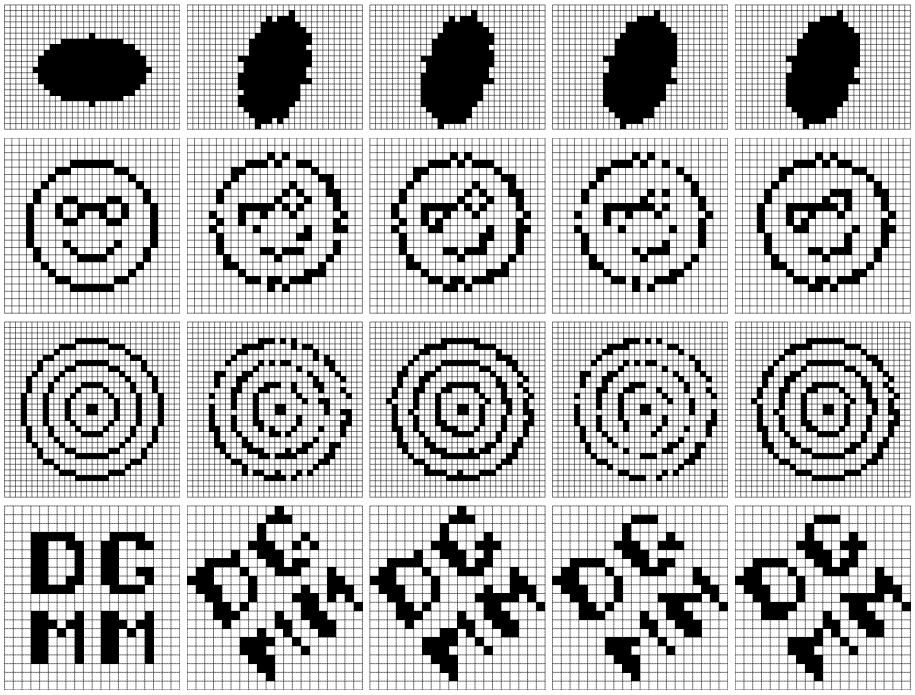

Fig. 3. Results of rigid motions in $\mathbb{Z}^2$. From left to right: input image X; usual Gaussian digitization of $\mathcal{R}(\square(\mathsf{X}))$ and its analogue version with our method (Eq. (14)); usual majority vote digitization of $\mathcal{R}(\square(\mathsf{X}))$ and its analogue version with our method (Eq. (15)). From top to bottom, the used rigid motion paramaters $(\alpha, \beta, t_x, t_y) \in \mathbb{Q}^4$ (Eq. (3)) are: $(\frac{22}{25}, \frac{7}{25}, 0, 0)$, $(\frac{5}{13}, \frac{12}{13}, \frac{1}{5}, \frac{2}{3})$, $(\frac{3}{5}, \frac{4}{5}, \frac{1}{3}, \frac{1}{3})$, $(\frac{3}{5}, \frac{4}{5}, \frac{1}{5}, \frac{1}{4})$.

optimization strategy under topological constraints. Since the definition of the final object is obtained by a constructive process, these topological constraints may lead to a non-convergence of the method when the structure of the object is too close to the resolution of the grid. A short term perspective will consist of considering multigrid strategies [4] to handle such cases.

As mid-term perspectives, we will also investigate our approach with other kinds of topological models (e.g. the well-composed sets [16]), but also with non-binary images [21]. Longer-term perspectives will consist of investigating transformations in higher dimensions [31, 33] and/or for richer families of transformations [8, 14, 18]. It would be also interesting to combine these topological constraints with other geometric constraints, such as minimizing perimeter and total curvature, and preserving convexity, etc.

References

1. Andres, É.: The quasi-shear rotation. In: DGCI. pp. 307–314 (1996)

2. Andres, É., Dutt, M., Biswas, A., Largeteau-Skapin, G., Zrour, R.: Digital two-dimensional bijective reflection and associated rotation. In: DGCI. pp. 3–14 (2019)
3. Anglin, W.S.: Using Pythagorean triangles to approximate angles. American Mathematical Monthly **95**(6), 540–541 (1988)
4. Bai, Y., Han, X., Prince, J.L.: Digital topology on adaptive octree grids. Journal of Mathematical Imaging and Vision **34**(2), 165–184 (2009)
5. Baudrier, É., Mazo, L.: Combinatorics of the Gauss digitization under translation in 2D. Journal of Mathematical Imaging and Vision **61**(2), 224–236 (2019)
6. Berthé, V., Nouvel, B.: Discrete rotations and symbolic dynamics. Theoretical Computer Science **380**(3), 276–285 (2007)
7. Bloch, I., Pescatore, J., Garnero, L.: A new characterization of simple elements in a tetrahedral mesh. Graphical Models **67**(4), 260–284 (2005)
8. Blot, V., Coeurjolly, D.: Quasi-affine transformation in higher dimension. In: DGCI. pp. 493–504 (2009)
9. Couprie, M., Bertrand, G.: New characterizations of simple points in 2D, 3D, and 4D discrete spaces. IEEE Trans. on Pattern Analysis and Machine Intelligence **31**(4), 637–648 (2009)
10. Damiand, G., Dupas, A., Lachaud, J.O.: Fully deformable 3D digital partition model with topological control. Pattern Recognition Letters **32**(9), 1374–1383 (2011)
11. Faisan, S., Passat, N., Noblet, V., Chabrier, R., Meyer, C.: Topology preserving warping of 3-D binary images according to continuous one-to-one mappings. IEEE Transactions on Image Processing **20**(8), 2135–2145 (2011)
12. Heijmans, H.J.A.M., Ronse, C.: The algebraic basis of mathematical morphology. I Dilations and erosions. Computer Vision, Graphics, and Image Processing **50**(3), 245–295 (1990)
13. Jacob, M.A., Andres, É.: On discrete rotations. In: DGCI. pp. 161–174 (1995)
14. Jacob-Da Col, M., Mazo, L.: nD quasi-affine transformations. In: DGCI. pp. 337–348 (2016)
15. Kovalevsky, V.A.: Finite topology as applied to image analysis. Computer Vision, Graphics, and Image Processing **46**(2), 141–161 (1989)
16. Latecki, L.J., Eckhardt, U., Rosenfeld, A.: Well-composed sets. Computer Vision and Image Understanding **61**(1), 70–83 (1995)
17. Mazo, L., Passat, N., Couprie, M., Ronse, C.: Paths, homotopy and reduction in digital images. Acta Applicandae Mathematicae **113**(2), 167–193 (2011)
18. Mazo, L.: Multi-scale arithmetization of linear transformations. Journal of Mathematical Imaging and Vision **61**(4), 432–442 (2019)
19. Mazo, L., Baudrier, É.: Object digitization up to a translation. Journal of Computer and System Sciences. **95**, 193–203 (2018)
20. Mazo, L., Passat, N., Couprie, M., Ronse, C.: Digital imaging: A unified topological framework. Journal of Mathematical Imaging and Vision **44**(1), 19–37 (2012)
21. Mazo, L., Passat, N., Couprie, M., Ronse, C.: Topology on digital label images. Journal of Mathematical Imaging and Vision **44**(3), 254–281 (2012)
22. Ngo, P., Kenmochi, Y., Passat, N., Talbot, H.: Combinatorial structure of rigid transformations in 2D digital images. Computer Vision and Image Understanding **117**(4), 393–408 (2013)
23. Ngo, P., Kenmochi, Y., Passat, N., Talbot, H.: Topology-preserving conditions for 2D digital images under rigid transformations. Journal of Mathematical Imaging and Vision **49**(2), 418–433 (2014)
24. Ngo, P., Passat, N., Kenmochi, Y., Debled-Rennesson, I.: Convexity invariance of voxel objects under rigid motions. In: ICPR. pp. 1157–1162 (2018)
25. Ngo, P., Passat, N., Kenmochi, Y., Debled-Rennesson, I.: Geometric preservation of 2D digital objects under rigid motions. Journal of Mathematical Imaging and Vision **61**(2), 204–223 (2019)

26. Ngo, P., Passat, N., Kenmochi, Y., Talbot, H.: Topology-preserving rigid transformation of 2D digital images. IEEE Transactions on Image Processing **23**(2), 885–897 (2014)
27. Nouvel, B., Rémila, E.: Characterization of bijective discretized rotations. In: IWCIA. pp. 248–259 (2004)
28. Nouvel, B., Rémila, E.: Incremental and transitive discrete rotations. In: IWCIA. pp. 199–213 (2006)
29. Passat, N., Kenmochi, Y., Ngo, P., Pluta, K.: Rigid motions in the cubic grid: A discussion on topological issues. In: DGCI. pp. 127–140 (2019)
30. Pluta, K., Moroz, G., Kenmochi, Y., Romon, P.: Quadric arrangement in classifying rigid motions of a 3D digital image. In: CASC. pp. 426–443 (2016)
31. Pluta, K., Romon, P., Kenmochi, Y., Passat, N.: Bijectivity certification of 3D digitized rotations. In: CTIC. pp. 30–41 (2016)
32. Pluta, K., Romon, P., Kenmochi, Y., Passat, N.: Bijective digitized rigid motions on subsets of the plane. Journal of Mathematical Imaging and Vision **59**(1), 84–105 (2017)
33. Richard, A., Fuchs, L., Largeteau-Skapin, G., Andres, É.: Decomposition of nD-rotations: Classification, properties and algorithm. Graphical Models **73**(6), 346–353 (2011)
34. Rosenfeld, A.: Adjacency in digital pictures. Information and Control **26**(1), 24–33 (1974)
35. Rosenfeld, A.: Digital topology. The American Mathematical Monthly **86**(8), 621–630 (1979)
36. Rosenfeld, A., Kong, T.Y., Nakamura, A.: Topology-preserving deformations of two-valued digital pictures. Graphical Models and Image Processing **60**(1), 24–34 (1998)
37. Roussillon, T., Coeurjolly, D.: Characterization of bijective discretized rotations by Gaussian integers. Tech. rep. (2016), https://hal.archives-ouvertes.fr/hal-01259826
38. Thibault, Y., Sugimoto, A., Kenmochi, Y.: 3D discrete rotations using hinge angles. Theoretical Computer Science **412**(15), 1378 – 1391 (2011)
39. Whitehead, J.H.C.: Simplicial spaces, nuclei and m-groups. Proceedings of the London Mathematical Society **s2-45**(1), 243–327 (1939)

A Construction of the cellular space $\mathbb{H}$

We describe hereafter the way we build the cellular space $\mathbb{H}$ that refines the two cubical spaces $\mathbb{F}$ and $\mathbb{G}$.

A.1 Input

Although $\mathbb{F}$, $\mathbb{G}$ and $\mathbb{H}$ are infinite spaces, our purpose is to handle finite digital objects. As a consequence, our first input is a finite subset S of $\mathbb{Z}^2$ that will include these digital objects. Without loss of generality, S is assumed to be a square $[\![-s, s]\!]^2 \subset \mathbb{Z}^2$ with $s \in \mathbb{N}^\star$. The continuous analogue of this digital set S is the Euclidean square subset of $\mathbb{R}^2$ defined as $S = \square(\mathsf{S}) = [-s - \frac{1}{2}, s + \frac{1}{2}]^2 \subset \mathbb{R}^2$.

The parameters that define the rigid motion $\mathcal{R}$ are also required, namely the values $\alpha = \frac{a}{c}, \beta = \frac{b}{c} \in \mathbb{Q}$ (with $(a, b, c) \subset \mathbb{Z}^3$ a Pythagorean triple) that define the rotation matrix; and the values $t_x, t_y \in \mathbb{Q}$ that define the translation vector $\mathbf{t}$ (see Eq. (4)).

Consequently, the information required as input is a 5-uple $(s, a, b, t_x, t_y) \in \mathbb{N}^\star \times \mathbb{Z}^2 \times \mathbb{Q}^2$ that satisfies $\sqrt{a^2 + b^2} \in \mathbb{N}$.

A.2 Output

The output of the algorithm is the finite subspace (namely a complex) of the cellular space $\mathbb{H}$ that intersects a Euclidean square $Q = [q_x, q_x + w] \times [q_y, q_y + w] \subset \mathbb{R}^2$, with $\mathbf{q} \in (\mathbb{Z} + \frac{1}{2})^2$ and $w \in \mathbb{N}^\star$. The position of Q (given by $\mathbf{q}$) mainly depends on the input translation vector $\mathbf{t}$. The size of Q (i.e. w) depends on the parameter s that conditions the size of the input square, and on the rotation angle deriving from a and b. (Note that we will have $2s+1 \leq w \leq (2s+1)\sqrt{2}+1$, i.e. the output square Q will always be larger than the input square S but not much larger.)

The output cellular space $\mathbb{H}(Q) = \{\mathfrak{h} \in \mathbb{H} \mid \mathfrak{h} \subset Q\}$ is defined as a finite set of faces of $\mathbb{H}$, and is partitioned into three subsets $\mathbb{H}_0(Q)$, $\mathbb{H}_1(Q)$ and $\mathbb{H}_2(Q)$ that contain the 0-, 1- and 2-faces of $\mathbb{H}(Q)$, respectively. In particular, $\mathbb{H}_0(Q) \cup \mathbb{H}_1(Q) \cup \mathbb{H}_2(Q) = \mathbb{H}(Q)$ is a partition of Q.

For each face $\mathfrak{h}$, we also compute the closure $C(\mathfrak{h})$ and/or the star $S(\mathfrak{h})$ within the subspace $\mathbb{H}(Q)$. If $\mathfrak{h}$ is a 0- (resp. 1-, resp. 2-) face, we compute $S_1(\mathfrak{h})$ and $S_2(\mathfrak{h})$ (resp. $C_0(\mathfrak{h})$ and $S_2(\mathfrak{h})$, resp. $C_0(\mathfrak{h})$ and $C_1(\mathfrak{h})$) where $S_d(\mathfrak{h})$ (resp. $C_d(\mathfrak{h})$) is the part of $S(\mathfrak{h})$ (resp. $C(\mathfrak{h})$) composed by the d-faces ($0 \leq d \leq 2$).

For each 2-face $\mathfrak{h}_2$, we also compute the functions ϕ and γ. More precisely, we compute the functions $\tilde{\phi}, \tilde{\gamma} : \mathbb{H}_2 \to \mathbb{Z}^2$ such that $\tilde{\phi}(\mathfrak{h}_2) = \boxdot(\phi(\mathfrak{h}_2))$ and $\tilde{\gamma}(\mathfrak{h}_2) = \boxdot(\mathcal{R}^{-1}(\gamma(\mathfrak{h}_2)))$. (This is indeed relevant since $\boxdot$ is a bijection between $\mathbb{F}_2$ and $\mathbb{Z}^2$ whereas $\boxdot \circ \mathcal{R}^{-1}$ is a bijection between $\mathbb{G}_2$ and $\mathbb{Z}^2$.) In particular, these functions allow us to define the two functions $\tilde{\Phi} : \boxdot(Q) \subset \mathbb{Z}^2 \to 2^{\mathbb{H}_2}$ and $\tilde{\Gamma} : \mathsf{S} \subset \mathbb{Z}^2 \to 2^{\mathbb{H}_2}$ such that for any $\mathbf{p} \in \phi(\mathbb{H}_2)$ (resp. $\mathbf{p} \in \mathsf{S}$), we have $\tilde{\Phi}(\mathbf{p}) = \tilde{\phi}^{-1}(\{\mathbf{p}\})$ (resp. $\tilde{\Gamma}(\mathbf{p}) = \tilde{\gamma}^{-1}(\{\mathbf{p}\})$).

A.3 Definition of the square Q

The first task is to define the square Q, i.e. to define $\mathbf{q}$ and w so that Q includes the image of the square S by the rigid motion $\mathcal{R}$. Since S is convex, we can simply compute the images of the four vertices of S by $\mathcal{R}$ to reach that goal. In particular, for $0 \leq i, j \leq 1$, we set:

$$\mathbf{c}^{i,j} = ((-1)^i(s + \frac{1}{2}), (-1)^j(s + \frac{1}{2})) \tag{16}$$

The four points $\mathbf{c}^{i,j}$ are the vertices of S. For $0 \leq i, j \leq 1$, we compute $\mathbf{r}^{i,j} = \mathcal{R}(\mathbf{c}^{i,j})$. We set:

$$r_x^- = \min_{i,j}\{\lfloor r_x^{i,j} + \frac{1}{2} \rfloor\} - \frac{1}{2} \qquad r_y^- = \min_{i,j}\{\lfloor r_y^{i,j} + \frac{1}{2} \rfloor\} - \frac{1}{2} \tag{17}$$

$$r_x^+ = \max_{i,j}\{\lceil r_x^{i,j} - \frac{1}{2} \rceil\} + \frac{1}{2} \qquad r_y^+ = \max_{i,j}\{\lceil r_y^{i,j} - \frac{1}{2} \rceil\} + \frac{1}{2} \tag{18}$$

Finally, we define:

$$q_x = r_x^- \quad q_y = r_y^- \tag{19}$$

$$w = \max\{r_x^+ - r_x^-, r_y^+ - r_y^-\} \tag{20}$$

The square Q is then defined by its four vertices $\mathbf{q}^{0,0} = \mathbf{q}$, $\mathbf{q}^{w,0} = \mathbf{q} + w\mathbf{e}_x$, $\mathbf{q}^{0,w} = \mathbf{q} + w\mathbf{e}_y$ and $\mathbf{q}^{w,w} = \mathbf{q} + w\mathbf{e}_x + w\mathbf{e}_y$

A.4 Definition of the generator lines of $\mathbb{H}(Q)$

The cellular subspace $\mathbb{H}(Q)$ is induced by the subdivision of Q by the lines of $\mathscr{V}_\Delta$, $\mathscr{H}_\Delta$, $\mathcal{R}(\mathscr{V}_\Delta)$ and $\mathcal{R}(\mathscr{H}_\Delta)$. These four sets are infinite, but for each of them, the subset of lines that contribute to the subdivision of Q is finite and corresponds to the lines that intersect the square Q. The subsets $\mathscr{V}_\Delta(Q)$ of $\mathscr{V}_\Delta$ and $\mathscr{H}_\Delta(Q)$ of $\mathscr{H}_\Delta$ are defined by:

$$\mathscr{V}_\Delta(Q) = \{V_\delta \mid \delta \in \Delta \cap [q_x, q_x + w]\} \tag{21}$$

$$\mathscr{H}_\Delta(Q) = \{H_\delta \mid \delta \in \Delta \cap [q_y, q_y + w]\} \tag{22}$$

whereas the subsets $\mathcal{R}(\mathscr{V}_\Delta)(Q)$ of $\mathcal{R}(\mathscr{V}_\Delta)$ and $\mathcal{R}(\mathscr{H}_\Delta)(Q)$ of $\mathcal{R}(\mathscr{H}_\Delta)$ can be determined as follows. For $0 \leq i, j \leq 1$, we compute:

$$\mathbf{u}^{i,j} = \mathcal{R}^{-1}(\mathbf{q}^{iw,jw}) \tag{23}$$

These four points $\mathbf{u}^{i,j}$ are the vertices of the square $\mathcal{R}^{-1}(Q)$. We set:

$$\delta_x^- = \min_{i,j}(\lceil u_x^{i,j} + \frac{1}{2} \rceil) - \frac{1}{2} \qquad \delta_x^+ = \max_{i,j}(\lfloor u_x^{i,j} - \frac{1}{2} \rfloor) + \frac{1}{2} \tag{24}$$

$$\delta_y^- = \min_{i,j}(\lceil u_y^{i,j} + \frac{1}{2} \rceil) - \frac{1}{2} \qquad \delta_y^+ = \max_{i,j}(\lfloor u_y^{i,j} - \frac{1}{2} \rfloor) + \frac{1}{2} \tag{25}$$

The only lines of $\mathscr{V}_\Delta$ (resp. $\mathscr{H}_\Delta$) that intersect $\mathcal{R}^{-1}(Q)$ are the lines V_δ (resp. H_δ) for $\delta_x^- \leq \delta \leq \delta_x^+$ (resp. $\delta_y^- \leq \delta \leq \delta_y^+$). This leads us to define the subsets $\mathcal{R}(\mathscr{V}_\Delta)(Q)$ of $\mathcal{R}(\mathscr{V}_\Delta)$ and $\mathcal{R}(\mathscr{H}_\Delta)(Q)$ of $\mathcal{R}(\mathscr{H}_\Delta)$ as follows:

$$\mathcal{R}(\mathscr{V}_\Delta)(Q) = \{\mathcal{R}(V_\delta) \mid \delta_x^- \leq \delta \leq \delta_x^+\} \tag{26}$$

$$\mathcal{R}(\mathscr{H}_\Delta)(Q) = \{\mathcal{R}(H_\delta) \mid \delta_y^- \leq \delta \leq \delta_y^+\} \tag{27}$$

A.5 Definition of $\mathbb{H}_\mathbf{0}(Q)$

Any 0-face $\mathfrak{f}_0$ of $\mathbb{H}(Q)$ corresponds to the intersection of (at least) two lines of $\mathscr{V}_\Delta(Q)$, $\mathscr{H}_\Delta(Q)$, $\mathcal{R}(\mathscr{V}_\Delta)(Q)$ and $\mathcal{R}(\mathscr{H}_\Delta)(Q)$ inside the square Q. (Of course, such two lines cannot belong to a same subset.) Reversely, two lines from two of these subsets can induce at most one such 0-face. In order to ensure that the intersection between two lines is indeed inside the square Q, we define for each line L the segment, noted $Q(L)$, that corresponds the intersection between L and Q. In particular, two lines L_1 and L_2 will intersect inside Q iff $Q(L_1)$ and $Q(L_2)$ intersect.

Let L be a line of $\mathscr{V}_\Delta(Q)$, $\mathscr{H}_\Delta(Q)$, $\mathcal{R}(\mathscr{V}_\Delta)(Q)$ or $\mathcal{R}(\mathscr{H}_\Delta)(Q)$. We compute the putative intersections $L \cap V_{q_x} = \{\mathbf{m}^{x-}\}$, $L \cap V_{q_x+w} = \{\mathbf{m}^{x+}\}$, $L \cap H_{q_y} = \{\mathbf{m}^{y-}\}$ and $L \cap H_{q_y+w} = \{\mathbf{m}^{y+}\}$ with the convention that $\mathbf{m}^{x-} = (m_x^{y-}, -\infty)$ and $\mathbf{m}^{x+} = (m_x^{y+}, +\infty)$ if L is colinear to V_{q_x} and V_{q_x+w} and $\mathbf{m}^{y-} = (-\infty, m_y^{x-})$ and $\mathbf{m}^{y+} = (+\infty, m_y^{x+})$ if L is colinear to H_{q_y} and H_{q_y+w}. The segment associated to L is then:

$$Q(L) = [(\max\{m_x^{x-}, m_x^{y-}\}, \max\{m_y^{x-}, m_y^{y-}\}), (\min\{m_x^{x+}, m_x^{y+}\}, \min\{m_y^{x+}, m_y^{y+}\})] \tag{28}$$

For the sake of concision, a 0-face $\mathfrak{f}_0$ will be also noted as $\langle \mathbf{h} \rangle$ where $\mathbf{h}$ is the point that defines this face, i.e. the intersection point of these two lines.

Let L_1, L_2 be two lines of two distinct subsets of $\mathscr{V}_\Delta(Q)$, $\mathscr{H}_\Delta(Q)$, $\mathcal{R}(\mathscr{V}_\Delta)(Q)$ or $\mathcal{R}(\mathscr{H}_\Delta)(Q)$. If $L_1 \cap L_2 = \{\mathbf{h}\}$ (i.e. if $L_1 \cap L_2 \neq \emptyset$ and $L_1 \neq L_2$, i.e. L_1, L_2 are non-colinear), then $\langle \mathbf{h} \rangle$ is a 0-face of $\mathbb{H}_0(Q)$ iff $\mathbf{h} \in Q(L_1)$ and $\mathbf{h} \in Q(L_2)$. The exhaustive scanning of all the couples of lines within $\mathscr{V}_\Delta(Q)$, $\mathscr{H}_\Delta(Q)$, $\mathcal{R}(\mathscr{V}_\Delta)(Q)$ or $\mathcal{R}(\mathscr{H}_\Delta)(Q)$ then allows us to build $\mathbb{H}_0(Q)$.

A.6 Definition of $\mathbb{H}_1(Q)$

For each line L of $\mathscr{V}_\Delta(Q)$, $\mathscr{H}_\Delta(Q)$, $\mathcal{R}(\mathscr{V}_\Delta)(Q)$ or $\mathcal{R}(\mathscr{H}_\Delta)(Q)$, we keep track of all the 0-faces of $\mathbb{H}_0(Q)$ induced by the intersection of L with another line. In particular, we note $I(L)$ the sets of all the points corresponding to these 0-faces.

For the sake of concision, a 1-face $\mathfrak{f}_1$ will be also noted as $\langle \mathbf{h}_1, \mathbf{h}_2 \rangle$ where $\mathfrak{f}_1 =]\mathbf{h}_1, \mathbf{h}_2[$.

Let $I(L) = \{\mathbf{h}_0, \dots, \mathbf{h}_i \dots, \mathbf{h}_t\}$ ($t \geq 0$). Without loss of generality, we assume that the points $\mathbf{h}_i$ are sorted in the lexicographic order in $\mathbb{Q}^2$. (Note that we have $\mathbf{h}_0$ and $\mathbf{h}_t$ equal to the bounds of $Q(L)$.) Then, for any $0 \leq i \leq t-1$, $\langle \mathbf{h}_i, \mathbf{h}_{i+1} \rangle$ is a 1-face of $\mathbb{H}_1(Q)$. Reversely, each 1-face of $\mathbb{H}_1(Q)$ satisfies this property for one (or two) line(s) L of $\mathscr{V}_\Delta(Q)$, $\mathscr{H}_\Delta(Q)$, $\mathcal{R}(\mathscr{V}_\Delta)(Q)$ or $\mathcal{R}(\mathscr{H}_\Delta)(Q)$.

For any 1-face $\mathfrak{f}_1 = \langle \mathbf{h}_i, \mathbf{h}_{i+1} \rangle$, the set $C_0(\mathfrak{f}_1)$ is defined as $\{\langle \mathbf{h}_i \rangle, \langle \mathbf{h}_{i+1} \rangle\}$. Reversely, for any 0-face $\mathfrak{f}_0 \in \mathbb{H}_0$, the set $S_1(\mathfrak{f}_0)$ is defined as $\{\mathfrak{f}_1 \in \mathbb{H}_1 \mid \mathfrak{f}_0 \in C_0(\mathfrak{f}_1)\}$.

A.7 Definition of $\mathbb{H}_2(Q)$

Let $\mathfrak{f}_0 = \langle \mathbf{h} \rangle$ be a 0-face of $\mathbb{H}_0$. The set $S_1(\mathfrak{f}_0)$ contains 2 to 8 1-faces $\langle \mathbf{h}, \mathbf{h}' \rangle$ that can be easily sorted in the clockwise order with respect to the orientation of the vectors $\mathbf{h}' - \mathbf{h}$. For each 1-face $\mathfrak{f}_1 = \langle \mathbf{h}, \mathbf{h}' \rangle$ of $\mathbb{H}_1$, we can then define the successor of $\mathfrak{f}_1$ in $S(\langle \mathbf{h} \rangle)$ (resp. in $S(\langle \mathbf{h}' \rangle)$) with respect to this ordering. This successor will be noted $\sigma(\langle \mathbf{h}', \mathbf{h} \rangle)$ (resp. $\sigma(\langle \mathbf{h}, \mathbf{h}' \rangle)$); note in particular that the order of $\mathbf{h}, \mathbf{h}'$ in the notation of σ will then be important in that case.

For the sake of concision, a 2-face $\mathfrak{f}_2$ will be also noted as $\langle \mathbf{h}_1, \dots, \mathbf{h}_i, \dots \mathbf{h}_t \rangle$ ($t \geq 3$) where the $\mathbf{h}_i$ are the vertices of the corresponding convex polygon, clockwise ordered. Each 2-face[1] $\mathfrak{f}_2$ is defined (up to circular permutations) by $\langle \mathbf{h}_1, \dots, \mathbf{h}_i, \dots \mathbf{h}_t \rangle$ such that for any $1 \leq i, j \leq t$, we have $\mathbf{h}_i \neq \mathbf{h}_j$, for any $1 \leq i \leq t-2$, we have $\sigma(\langle \mathbf{h}_i, \mathbf{h}_{i+1} \rangle) = \langle \mathbf{h}_{i+1}, \mathbf{h}_{i+2} \rangle$ and $\sigma(\langle \mathbf{h}_{t-1}, \mathbf{h}_t \rangle) = \langle \mathbf{h}_t, \mathbf{h}_1 \rangle$.

For any 2-face $\mathfrak{f}_2 = \langle \mathbf{h}_1, \dots, \mathbf{h}_i, \dots \mathbf{h}_t \rangle$, the set $C_0(\mathfrak{f}_2)$ (resp. $C_1(\mathfrak{f}_2)$) is defined as $\{\langle \mathbf{h}_1 \rangle, \dots, \langle \mathbf{h}_i \rangle, \dots \langle \mathbf{h}_t \rangle\}$ (resp. $\{\langle \mathbf{h}_1, \mathbf{h}_2 \rangle, \dots, \langle \mathbf{h}_i, \mathbf{h}_{i+1} \rangle, \dots, \langle \mathbf{h}_{t-1}, \mathbf{h}_t \rangle, \langle \mathbf{h}_t, \mathbf{h}_1 \rangle\}$). Reversely, for any 0-face $\mathfrak{f}_0 \in \mathbb{H}_0$, the set $S_1(\mathfrak{f}_0)$ (resp. $S_2(\mathfrak{f}_0)$) is defined as $\{\mathfrak{f}_2 \in \mathbb{H}_2 \mid \mathfrak{f}_0 \in C_0(\mathfrak{f}_2)\}$ (resp. $\{\mathfrak{f}_2 \in \mathbb{H}_2 \mid \mathfrak{f}_1 \in C_1(\mathfrak{f}_2)\}$).

[1] There exists one such $\langle \mathbf{h}_1, \dots, \mathbf{h}_i, \dots \mathbf{h}_t \rangle$ which is not a 2-face, and that corresponds to the boundary of $\mathbb{H}(Q)$. It is characterized by the fact that it contains the four points $\mathbf{q}^{0,0}$, $\mathbf{q}^{w,0}$, $\mathbf{q}^{0,w}$ and $\mathbf{q}^{w,w}$.

A.8 Definition of the functions $\tilde{\phi}$, $\tilde{\gamma}$, $\tilde{\Phi}$, $\tilde{\Gamma}$

Let $\mathfrak{f}_2 = \langle \mathbf{h}_1, \ldots, \mathbf{h}_i, \ldots \mathbf{h}_t \rangle$ be a 2-face of $\mathbb{H}(Q)$. We set $\mathbf{b}(\mathfrak{f}_2)$ the barycentre of $\mathfrak{f}_2$ (simply computed[2] as $\mathbf{b}(\mathfrak{f}_2) = \frac{1}{t} \sum_{i=1}^{t} \mathbf{h}_i$). We set $\mathbf{a} = \mathcal{R}^{-1}(\mathbf{b}(\mathfrak{f}_2)$. We set:

$$\tilde{\phi}(\mathfrak{f}_2) = \arg_{\mathbf{p} \in \mathbb{Z}^2} \min \|\mathbf{p} - \mathbf{b}(\mathfrak{f}_2)\| = ([b_x(\mathfrak{f}_2)], [b_y(\mathfrak{f}_2)]) \tag{29}$$

and

$$\tilde{\gamma}(\mathfrak{f}_2) = \arg_{\mathbf{p} \in \mathbb{Z}^2} \min \|\mathbf{p} - \mathcal{R}^{-1}(\mathbf{b}(\mathfrak{f}_2))\| = ([a_x], [a_y]) \tag{30}$$

where $[\cdot]$ is the rounding operator. From $\tilde{\phi}$ and $\tilde{\gamma}$, we then define $\tilde{\Phi} : \tilde{\phi}(\mathbb{H}_2) \subset \mathbb{Z}^2 \to 2^{\mathbb{H}_2}$ and $\tilde{\Gamma} : \mathsf{S} \subset \mathbb{Z}^2 \to 2^{\mathbb{H}_2}$.

In particular, these functions allow us to define the two functions $\tilde{\Phi} : \tilde{\phi}(\mathbb{H}_2) \subset \mathbb{Z}^2 \to 2^{\mathbb{H}_2}$ and $\tilde{\Gamma} : \mathsf{S} \subset \mathbb{Z}^2 \to 2^{\mathbb{H}_2}$ as follows:

$$\forall \mathbf{p} \in \boxdot(Q), \forall \mathfrak{f}_2 \in \mathbb{H}_2, \mathfrak{f}_2 \in \tilde{\Phi}(\mathbf{p}) \Leftrightarrow \tilde{\phi}(\mathfrak{f}_2) = \mathbf{p} \tag{31}$$

and

$$\forall \mathbf{p} \in \mathsf{S}, \forall \mathfrak{f}_2 \in \mathbb{H}_2, \mathfrak{f}_2 \in \tilde{\Gamma}(\mathbf{p}) \Leftrightarrow \tilde{\gamma}(\mathfrak{f}_2) = \mathbf{p} \tag{32}$$

[2] In practice, considering any 3 points $\mathbf{h}_i$ would be enough for our purpose.